Inorg. Chem. **1987**, *26*, 259–265

Contribution from the Department of Chemistry, D-006, University of California at San Diego, La Jolla, California 92093,
and Department of Chemistry, University of Delaware, Newark, Delaware 19716

Syntheses of Photoactive Complexes. Electronic Spectra, Electrochemistry, and SCF–Xα–DV Calculations for Bis(phosphine)palladium Oxalate and Dithiooxalate Complexes. Crystal and Molecular Structures of (Dithiooxalato-*S*,*S'*)bis(trimethylphosphine)palladium(II) and (1,1-Dithiooxalato-*S*,*S'*)bis(μ_3-sulfido)-2,2,3,3-tetrakis(trimethylphosphine)-*triangulo*-tripalladium(II)

Robert L. Cowan,[1a] Daniel B. Pourreau,[1b] Arnold L. Rheingold,*[1c] Steven J. Geib,[1c]
and William C. Trogler*[1a]

Received July 25, 1986

The compounds $M(S_2C_2O_2)L_2$ (M = Ni, Pd, Pt; L = $P(CH_3)_3$ (PMe_3) or L_2 = $[P(C_6H_5)_2CH_2]_2$ (dppe), $[P(C_2H_5)_2CH_2]_2$ (depe)) were prepared from the reaction between $K_2S_2C_2O_2$ and MCl_2L_2 (M = Ni, Pd, Pt; L = depe, dppe), except for $NiCl_2(PMe_3)_2$, which was prepared from $NiCl_2$(1,2-dimethoxyethane), $K_2S_2C_2O_2$, and PMe_3. In all complexes the dithiooxalate ligand chelates through both sulfur atoms as evidenced by $\nu_{C=O}$ = 1632–1640 cm^{-1} for the uncomplexed carbonyl groups in the solution IR spectra. Crystals of $Pd(S_2C_2O_2)(PMe_3)_2$ belong to the space group *Pbca* with a = 13.479 (2) Å, b = 12.488 (2) Å, c = 17.542 (2) Å, Z = 8, and V = 2952.7 (7) Å^3. Solution of the structure by direct methods led to final values of R_F = 2.63 and R_{wF} = 3.23 with 137 least-squares parameters for 2159 unique reflections with $F_o > 5\sigma(F_o)$. The structure confirmed the square-planar structure about Pd with Pd–P = 2.294 (1) and 2.307 (1) Å and Pd–S = 2.324 (1) and 2.344 (1) Å. All dithiooxalate complexes were photoactive and liberated carbonyl sulfide and products derived from ML_2 on photolysis. Thermolysis of $Pd(S_2C_2O_2)(PMe_3)_2$ in DMF produced crystals of $Pd_3(\mu_3\text{-}S)_2(S_2C_2O_2)(PMe_3)_4$ on cooling that belong to the space group $P2_1$ with a = 9.580 (2) Å, b = 11.578 (2) Å, c = 13.400 (4) Å, β = 96.93 (2)°, Z = 2, and V = 1475.4 (4) Å^3. Solution of the structure by direct methods led to final values of R_F = 2.50 and R_{wF} = 2.82 with 245 least-squares parameters for 2523 unique reflections with $F_o > 5\sigma(F_o)$. The molecular structure consists of a triangle of palladium atoms with Pd(1)–Pd(2) = 3.174 (1) Å, Pd(1)–Pd(3) = 3.038 (1) Å, and Pd(2)–Pd(3) = 3.141 (1) Å capped above and below the plane by sulfurs Pd(1)–S(1) = 2.364 (2) Å, Pd(1)–S(2) = 2.374 (2) Å, Pd(2)–S(1) = 2.356 (2) Å, Pd(2)–S(2) = 2.353 (2) Å, Pd(3)–S(1) = 2.333 (2) Å, and Pd(3)–S(2) = 2.339(2) Å. The coordination geometry, including the capping sulfides, about each palladium is pseudo square planar with Pd(1) and Pd(2) each binding two PMe_3 ligands and Pd(3) binding to a dithiooxalate-*S*,*S'* ligand. SCF–Xα–DV calculations for the model complexes $Pd(C_2O_4)(PH_3)_2$ and $Pd(S_2C_2O_2)(PH_3)_2$ show a similar orbital energy scheme. The lowest energy and presumably photoactive electronic transitions are to empty $C_2O_4^{2-}$ and $S_2C_2O_2^{2-}$ π^* orbitals rather than to a ligand to metal charge-transfer transition. Several of the dithiooxalate complexes prepared showed chemically reversible reductions at −1.5 to −1.6 V in CH_3CN vs. Ag/AgCl, while all analogous oxalate complexes showed irreversible reductions at −1.5 to −2.1 V.

Introduction

Group 10 transition-metal bis(phosphine) oxalate compounds undergo photochemical conversion to the corresponding ML_2 species (L = PR_3) (eq 1).[2] This has been observed for M = Pt and Pd; however, we have found the analogous oxalate complexes of nickel difficult to prepare. Presumably the instability of bis(phosphine)nickel oxalates reflects the inability of Ni(II) to support a cis square-planar geometry with sterically demanding phosphine ligands, and a weak-field oxalate ligand. To photochemically generate the NiL_2 species we therefore prepared complexes containing the dithiooxalate-*S*,*S'* ligand for the entire series Ni, Pd, and Pt. Photoreductive elimination of dithiooxalate could be a novel method for generating COS within the coordination sphere of a low-valent metal. Dithiooxalate complexes that are bound through sulfur usually contain a hard metal ion chelated to the oxygens or else bridge two metal centers.[3] There is a report of $Ni(S_2C_2O_2)$(dppe),[4] where dppe = 1,2-bis(diphenylphosphino)ethane; however, only elemental analyses were given, and the mode of dithiooxalate binding was not characterized. The reported[4] synthesis (in dichloromethane solvent) failed to give any product in our hands, but yields product in methanol solvent. Because of the paucity of characterized mononuclear dithiooxalate-*S*,*S'* complexes we report crystallographic, theoretical, and spectroscopic studies for these complexes.

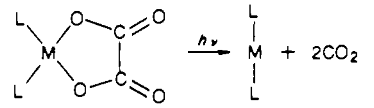

(1)

Experimental Section

Materials. Acetonitrile and dichloromethane were refluxed under nitrogen and distilled from CaH_2 before use. Pentane, THF, benzene, and diethyl ether were refluxed under nitrogen and distilled from sodium or potassium benzophenone ketyl. Other solvents were reagent grade and were used after degassing with a N_2 purge. The compounds dppe (1,2-bis(diphenylphosphino)ethane), trimethylphosphine, and triphenylphosphine (Strem), K_2PtCl_4 and $PdCl_2$ (Englehard), carbonyl sulfide (Matheson), Ni(DME)Cl_2 and Ni(dppe)$(CO)_2$ (Alfa) and Et_2S and benzonitrile (bzn) (Aldrich) were used as received. The compounds *cis*-$PtCl_2(Et_2S)_2$,[5] *trans*-$PdCl_2(bzn)_2$,[6] $K_2S_2C_2O_2$,[7] and depe (1,2-bis(diethylphosphino)ethane)[8] were all synthesized according to literature procedures. Potassium dithiooxalate must be prepared shortly before use since the ordinarily white powder decomposes to brown within a period of 6 months. Commercial sources of the compound were of poor or variable quality and are not recommended. The $MCl_2(PMe_3)_2$ complexes (M = Pt, Pd) were prepared by ligand displacement of SEt_2 or bzn with PMe_3. The $PtCl_2$(diphosphine) and $PdCl_2$(diphosphine) complexes were prepared by the method of Booth and Chatt[9a] in boiling DMF solvent. The $NiCl_2$(diphosphine) complexes were prepared from $NiCl_2 \cdot 2H_2O$ and the appropriate ligand in absolute ethanol solvent. All palladium and platinum phosphine dichloride and dithiooxalate complexes were best recrystallized from hot DMF. The nickel complexes were best recrystallized from CH_3CN/Et_2O solvent mixtures. Elemental analyses were performed by Galbraith Laboratories, Inc.

---

(1) (a) University of California at San Diego. (b) Present address: Department of Chemistry, The Pennsylvania State University, University Park, PA 16802. (c) University of Delaware.

(2) Paonessa, R. S.; Prignano, A. L.; Trogler, W. C. *Organometallics* **1982**, *4*, 647.

(3) (a) Coucouvanis, D. *Trans. Metal Chem., Proc. Workshop, 1980* **1981**, 59. (b) Leitheiser, M.; Coucouvanis, D. *Inorg. Chem.* **1977**, *16*, 1611. (c) Golič, L.; Bulc, N.; Dietzsch, W. *Inorg. Chem.* **1982**, *21*, 3560. (d) Dietzsch, W.; Bulc, N.; Golič, L.; Šiftar, J. *Z. Chem.* **1981**, *21*, 269. (e) Golič, L.; Bulc, N.; Dietzsch, W. *Polyhedron* **1983**, *2*, 1201.

(4) Bowmaker, G. A.; Boyd, P. D. W.; Campbell, G. K. *Inorg. Chem.* **1982**, *21*, 2403.

(5) Pidcock, A. L. *Inorg. Synth.* **1960**, *6*, 211.

(6) Doyle, J. R.; Slade, P. E.; Jonassen, H. B. *Inorg. Synth.* **1960**, *6*, 218.

(7) Jones, H. O.; Tasker, H. S. *J. Chem. Soc.* **1909**, *95*, 1904.

(8) Burt, R. J.; Chatt, J.; Hussain, W.; Leigh, G. J. *J. Organomet. Chem.* **1979**, *182*, 203.

(9) (a) Booth, G.; Chatt, J. *J. Chem. Soc.* **1965**, 3238. (b) Geary, W. J. *Coord. Chem. Rev.* **1971**, *7*, 81.

0020-1669/87/1326-0259$01.50/0 © 1987 American Chemical Society

Instrumentation. UV–vis spectra were recorded on an IBM Model 9420 spectrophotometer in matched 1-cm quartz cuvettes. Irradiations were performed with the use of a 450-W Hanovia medium-pressure mercury arc lamp contained within a water-cooled quartz jacket. Preparative scale photolyses were performed in a quartz Schlenk tube of about 50-mL volume. Solution IR spectra were taken with either a Perkin-Elmer 1320 spectrometer or an IBM IR/32 FTIR spectrometer in matched 0.1-mm CaF_2 cells. Low-temperature IR spectra were taken with use of a NaCl liquid cell mounted in a Specac P/N 21,000 variable-temperature Dewar.

All ^{31}P NMR spectra were taken with use of a Nicolet 200 (80.988 MHz) FT spectrometer. Chemical shifts (at 23 °C) were referenced to the deuterated solvent lock, which in turn had been previously calibrated against 85% H_3PO_4. All shifts are recorded relative to H_3PO_4 with downfield shifts being positive. The notation (^1H) denotes broad-band noise decoupling of the hydrogen nuclei.

(1,2-Bis(diethylphosphino)ethane)(dithiooxalato-*S,S'*)nickel(II), $Ni(S_2C_2O_2)$(depe). Procedure A: A suspension of $NiCl_2$(depe) (0.107 g, 0.32 mmol) and $K_2S_2C_2O_2$ (0.067 g, 0.34 mmol) in 10 mL of degassed MeOH were stirred under an atmosphere of nitrogen for 2 h. The resulting yellow suspension was cooled on an ice bath and filtered, and the resulting solid was then washed with ~5 mL of cold MeOH. Yield 0.098 g (80%). Anal. Calcd for $C_{12}H_{24}NiO_2P_2S_2$: C, 37.43; H, 6.28. Found: C, 37.45; H, 6.05.

(1,2-Bis(diethylphosphino)ethane)(dithiooxalato-*S,S'*)palladium(II), $Pd(S_2C_2O_2)$(depe). Procedure B: A solution of excess $K_2S_2C_2O_2$ (0.985 g, 4.97 mmol) in 10 mL of degassed H_2O was added to a suspension of $PdCl_2$(depe) (0.935 g, 2.44 mmol) and stirred for 2 h under an atmosphere of nitrogen. The resulting solution containing a yellow precipitate was cooled with an ice bath and filtered, and the resulting solid was washed with 5 mL of cold H_2O, 10 mL of cold MeOH, and 5 mL of Et_2O and dried in vacuo. Yield: 0.61 g (57%). Anal. Calcd for $C_{12}H_{24}O_2P_2PdS_2$: C, 33.30; H, 5.59. Found: C, 33.41; H, 5.60.

(1,2-Bis(diethylphosphino)ethane)(dithiooxalato-*S,S'*)platinum(II), $Pt(S_2C_2O_2)$(depe). Follow procedure B above using $K_2S_2C_2O_2$ (1.01 g, 5.10 mmol) and $PtCl_2$(depe) (1.00 g, 2.13 mmol). Yield: 0.85 g (77%). Anal. Calcd for $C_{12}H_{24}O_2P_2PtS_2$: C, 27.64; H, 4.65. Found: C, 27.56; H, 4.73.

(1,2-Bis(diphenylphosphino)ethane)(dithiooxalato-*S,S'*)nickel(II), $Ni(S_2C_2O_2)$(dppe). Follow procedure A with $NiCl_2$(dppe) (5.29 g, 10.0 mmol) and $K_2S_2C_2O_2$ (1.70 g, 8.57 mmol) in 500 mL of MeOH. Yield: 4.59 g, (75%). Anal. Calcd for $C_{28}H_{24}NiO_2P_2S_2$: C, 58.26; H, 4.19; S, 11.11. Found: C, 58.09; H, 4.30; S, 11.05.

(1,2-Bis(diphenylphosphino)ethane)(dithiooxalato-*S,S'*)palladium(II), $Pd(S_2C_2O_2)$(dppe). Follow procedure A using $PdCl_2$(dppe) (4.61 g, 8.01 mmol) and $K_2S_2C_2O_2$ (1.59 g, 8.02 mmol) in 400 mL of MeOH. Yield: 4.70 g (94%). Anal. Calcd for $C_{28}H_{24}O_2P_2PdS_2$: C, 53.81; H, 3.87; S, 10.26. Found: C, 52.83; H, 3.94; S, 9.94.

(1,2-Bis(diphenylphosphino)ethane)(dithiooxalato-*S,S'*)platinum(II), $Pt(S_2C_2O_2)$(diphos). Follow procedure A using $PtCl_2$(dppe) (2.66 g, 4.00 mmol) and $K_2S_2C_2O_2$ (0.793 g, 4.00 mmol) in 200 mL of MeOH. Yield: 2.47 g (86%). Anal. Calcd for $C_{28}H_{24}O_2P_2PtS_2$: C, 47.12; H, 3.39; S, 8.99. Found: C, 46.91; H, 3.47; S, 8.88.

Bis(trimethylphosphine)(dithiooxalato-*S,S'*)palladium(II), $Pd(S_2C_2O_2)(PMe_3)_2$. Follow procedure B using *trans*-$PdCl_2(PMe_3)_2$ (0.507 g, 1.54 mmol) and $K_2S_2C_2O_2$ (0.307 g, 1.55 mmol) in 10 mL of H_2O. Yield: 0.43 g (74%): Anal. Calcd for $C_8H_{18}O_2P_2PdS_2$: C, 25.37; H, 4.80. Found: C, 25.50; H, 4.93.

Bis(trimethylphosphine)(dithiooxalato-*S,S'*)platinum(II), $Pt(S_2C_2O_2)(PMe_3)_2$. Follow procedure B using *cis*-$PtCl_2(PMe_3)_2$ (10.51 g, 1.21 mmol) and $K_2S_2C_2O_2$ (0.241 g, 1.21 mmol) in 10 mL of H_2O. Yield: 0.48 g (85%): Anal. Calcd for $C_8H_{18}O_2P_2PtS_2$: C, 20.56; H, 3.89. Found: C, 20.47; H, 3.94.

Bis(trimethylphosphine)(dithiooxalato-*S,S'*)nickel(II), $Ni(S_2C_2O_2)(PMe_3)_2$. A suspension of $K_2S_2C_2O_2$ (0.90 g, 4.5 mmol) and $NiCl_2$(DME) (1.00 g, 4.5 mmol) in 20 mL of EtOH was stirred for 2 h under an atmosphere of nitrogen. The solution was cooled in an ice bath and filtered, and the crude product was dried in vacuo. This complex was dissolved in 15 mL of CH_2Cl_2 and PMe_3 (0.685 g, 0.91 mL, 9.0 mmol) was added drop by drop with stirring. The solution changed color from purple to dark red. Addition of 20 mL of Et_2O to this solution caused precipitation of a red-brown solid. Yield: 0.87 g (58%): Anal. Calcd for $C_8H_{18}NiO_2P_2$: C, 29.02; H, 5.48. Found: C, 28.43; H, 5.01. It should be noted that use of procedure A or B, starting with $NiCl_2(PMe_3)_2$ and $K_2S_2C_2O_2$, yielded $Ni(S_2C_2O_2)_2$ and not the desired product.

Photochemical Reactions of $Ni(S_2C_2O_2)L$ Complexes (L = dppe, depe) under a N_2 Atmosphere. The nickel complex was loaded into a quartz tube containing a stir bar and vacuum/N_2 cycled to remove air. Then 20 mL of distilled CH_3CN was added and the contents stirred vigorously to dissolve as much of the complex as possible. This solution was then exposed to the unfiltered light of the Hg arc lamp for 6–12 h. The photolysis mixture was then filtered through activated charcoal and Celite, using standard Schlenk techniques to exclude oxygen. This treatment removed most of the color in the photolysis mixture (presumably the color arises from cluster products), and solvent was removed in vacuo. The residue, dissolved in a minimum amount of THF, was layered with pentane to precipitate a brown solid and leave a clear solution on filtration. Evaporation of solvent yielded the nickel carbonyl complex as a solid residue.

Photochemical Reactions of $Ni(S_2C_2O_2)$(depe), $Pd(S_2C_2O_2)(PMe_3)_2$, and $Pt(S_2C_2O_2)(PMe_3)_2$ in Dichloromethane. Using a procedure similar to that above except substituting CH_2Cl_2 for the CH_3CN solvent and photolyzing for 2–3 days resulted in a red solution. Filtration of this photolysis mixture through activated charcoal and celite removed most of the red coloration. Concentration of the CH_2Cl_2 solution to ~5 mL and addition of 10–20 mL of diethyl ether or pentane completed the precipitation of MCl_2L_2 complexes, which were collected by filtration. If the photolysis solution was constantly purged with N_2, very little red coloration took place and the reaction yield increased to 90–100%.

Photolyses of $M(S_2C_2O_2)L_2$ Monitored by IR Spectroscopy. A saturated solution of the metal dithiooxalate compound in either CH_3CN or CH_2Cl_2 solution was loaded into a CaF_2 IR cell. With the use of a solvent reference, the spectrum of the starting solution was recorded. The IR cell was then placed in front of the mercury arc lamp for period of time varying from an initial 15 s to a final 5–10 min, and sequential spectra were recorded.

Photolyses Monitored by UV–Visible Absorption Spectroscopy. A ~10^{-5} M solution of the various metal dithiooxalate compounds in either CH_3CN or CH_2Cl_2 solvent was placed into a quartz cuvette and photolyzed with unfiltered light from the water-filtered mercury arc lamp for 30 s to 20 min.

Low-Temperature Photolyses of $M(S_2C_2O_2)L_2$ Complexes. A solution of the metal dithiooxalate compound in either CH_3CN or CH_2Cl_2 was loaded into a NaCl solution IR cell. This was then placed inside a Specac low-temperature Dewar. The Dewar was purged with dry N_2, partially evacuated, and cooled to −70 °C with a dry ice/acetone slush bath. At least $^1/_2$ h was allowed for the temperature to equilibrate before photolysis was begun. For some samples the Dewar was allowed to warm slowly to room temperature after photolysis with continuous monitoring by IR spectroscopy.

Photolyses of $M(S_2C_2O_2)L_2$ Complexes Monitored by ^{31}P NMR Spectroscopy. About 50 mg of metal dithiooxalate compound was put into a 10-mm NMR tube that was purged with N_2 and capped with a rubber septum. Then 2 mL of CD_3CN was added to dissolve the sample. The NMR tube containing sample was cooled to 0 °C and irradiated. Alternatively, the samples were irradiated in a quartz Schlenk tube, aliquots were withdrawn and put into a 10-mm NMR tube, and deuterated solvent was added for an NMR lock signal. Samples were then analyzed by ^{31}P NMR spectroscopy for percent conversion to products.

Thermal Reaction between $Ni(diphos)_2$ or $Ni(depe)_2$ and COS. In a nitrogen-filled glovebox a 50-mL Schlenk flask was loaded with a stir bar and 0.50 g of nickel complex. The flask was capped and 25 mL of dry distilled acetone was added under N_2. The slurry was stirred vigorously to dissolve as much of the nickel complex as possible before COS gas was bubbled through the solution (for about $^1/_2$ h). During addition of COS the solution changed from golden brown to red-orange. Attempts to remove the solvent in vacuo or to precipitate the product led to decomposition.

Electrochemical Determinations. Electrochemical measurements were made with an IBM EC/225 voltammetric analyzer employing a three-electrode cell consisting of a Pt-disk working electrode, Pt-wire auxiliary electrode, and a Ag/AgCl reference electrode. All voltammograms were taken of a 1 mM solution of the complex in dry degassed CH_3CN containing 0.1 M $(NBu_4)ClO_4$ as supporting electrolyte under a nitrogen atmosphere.

Electrical Conductivity Measurements. All conductivity measurements were made with an electric eye conductivity bridge Model RC 16B2 from Industrial Instruments, Inc. A 1 mM solution of the complex in acetone was loaded into the conductivity cell, and measurements were taken. The complexes analyzed include $Ni(S_2C_2O_2)$(dppe), $Pd(S_2C_2O_2)$(dppe), $Pt(S_2C_2O_2)$(dppe), and $Ni(S_2C_2O_2)$(depe). In all cases the Λ_m values measured were between 0.4 and 1.7. This low value indicates no appreciable ionization of the complexes, since the presence of two ions would require[9b] $\Lambda_m \sim 100$.

Crystal Structure Determinations for $[Pd(S_2C_2O_2)(PMe_3)_2]$ (I) and $[Pd_3(\mu_3\text{-}S)_2(S_2C_2O_2)(PMe_3)_4]$ (II). Large crystals of I can be grown by slow cooling of a hot saturated solution of the complex in DMF. It crystallizes as bright yellow plates with a few crystals thick enough to allow X-ray structure determination. If the solution of I is subjected to several heating and cooling cycles, thermolysis of complex I occurs and

Table I. Crystal, Data Collection, and Refinement Parameters for I and II

	I	II
formula	$C_8H_{18}O_2P_2S_2Pd$	$C_{14}H_{36}O_2P_4S_4Pd_3$
cryst system	orthorhombic	monoclinic
space group	*Pbca*	$P2_1$
a, Å	13.479 (2)	9.580 (2)
b, Å	12.488 (2)	11.578 (2)
c, Å	17.542 (2)	13.400 (4)
β, deg	90	96.93 (2)
V, Å^3	2952.7 (7)	1475.4 (4)
Z	8	2
D(calcd), g cm^{-3}	1.704	1.818
temp, °C	24	24
cryst dimens, mm	0.20 × 0.30 × 0.40	0.18 × 0.32 × 0.40
radiation	*a*	*a*
diffractometer	*b*	*b*
abs coeff, cm^{-1}	17.0	22.6
T(max)/*T*(min)	0.256/0.235	0.284/0.241
scan; speed, deg/min	variable; 7–20	variable; 10–20
2θ scan range, deg	4–50	4–50
scan technique	ω	Wyckoff
no. of unique data	2602 (2953 collected)	2740 (2861 collected)
no. of unique data with $(F_o) > 5\sigma(F_o)$	2159	2523
std reflecns	*c*	*c*
data/param ratio[d]	2159/137	2523/245
GOF	0.993	0.836
R_F, %	2.63	2.50
R_{wF}, %	3.23	2.82
weighting factor,[e] g	0.001	0.001

[a] Graphite monochromated Mo K_α (λ = 0.71073 Å). [b] Nicolet R3m/μ. [c] Three standards for every 197 reflections. [d] Reflections/least-squares parameters. [e] $w^{-1} = \sigma^2(F_o) + gF_o^2$.

on crystallization orange needles of II could be hand separated from the plates of complex I. The parameters used during the collection and refinement of diffraction data for $C_8H_{18}O_2P_2S_2Pd$ (I) and $C_{14}H_{36}O_2P_4S_4Pd_3$ (II) are given in Table I. Epoxy cement was used to attach a yellow crystal of I and an orange crystal of II to fine glass fibers. Systematic absences in the diffraction data prove that I crystallizes in the orthorhombic space group *Pbca* and that II crystallizes in either of the monoclinic space groups $P2_1$ or $P2_1/m$. The noncentrosymmetric space group, $P2_1$, was initially suggested by *E* statistics and later confirmed by the chemically reasonable solution and refinement of the structure. Unit cell dimensions were derived from the angular settings of 25 reflections with 20° ≤ 2θ ≤ 30° for I and II. Intensity data were corrected for absorption by an empirical procedure that employs six refined parameters to define a pseudoellipsoid used to calculate the corrections. A profile fitting procedure was applied to all intensity data to improve the precision of weak reflections.

Both structures were solved via the direct methods program SOLV, which in both cases located the Pd atoms. Remaining non-hydrogen atoms were found in subsequent difference Fourier syntheses and were refined anisotropically. Idealized hydrogen atom positions were calculated [*d*(C–H) = 0.96 Å; thermal parameters equal 1.2 times the isotropic equivalent for the carbon to which it was attached]. The final difference Fourier syntheses showed only a diffuse background (maximum contour: I, 0.40 e/Å^3; II, 0.63 e/Å^3). Refinement of a multiplicative factor for $\Delta f''$ shows that the reported coordinates are the preferred enantiomorph for II (η = 1.07 (8)). An inspection of F_o vs. F_c values and trends based on sin θ, Miller index, or parity group for both I and II did not show systematic errors in the data for either compound. All computer programs used in the data collection and refinements are contained in the Nicolet program packages P3, SHELXTL (version 5.1) and XP (Nicolet XRD, Madison, WI).

Tables II and III provide the atomic coordinates for I and II, respectively. Selected bond distances and angles for I and II are given in Tables IV and V. Additional crystallographic data are available (see supplementary material available paragraph at the end of the paper).

Table II. Atomic Coordinates (×10^4) and Isotropic Thermal Parameters (Å^2 × 10^3) for $Pd(S_2C_2O_2)(PMe_3)_2$

	x	*y*	*z*	U^a
Pd	904 (1)	1267 (1)	482 (1)	34 (1)
S(1)	717 (1)	1497 (1)	−825 (1)	60 (1)
S(2)	2032 (1)	−111 (1)	214 (1)	53 (1)
P(1)	−85 (1)	2736 (1)	681 (1)	42 (1)
P(2)	1235 (1)	976 (1)	1756 (1)	40 (1)
O(1)	1544 (3)	464 (3)	−1933 (2)	89 (1)
O(2)	3016 (2)	−362 (3)	−1052 (2)	70 (1)
C(1)	1531 (3)	627 (4)	−1248 (2)	49 (1)
C(2)	2290 (3)	23 (3)	−749 (2)	47 (1)
C(3)	−474 (4)	3430 (4)	−172 (3)	81 (2)
C(4)	−1254 (3)	2502 (4)	1165 (3)	58 (1)
C(5)	508 (4)	3810 (3)	1205 (3)	64 (2)
C(6)	415 (4)	1420 (4)	2508 (2)	70 (2)
C(7)	2416 (4)	1571 (4)	2002 (3)	78 (2)
C(8)	1379 (3)	−427 (3)	2010 (2)	62 (2)

[a] Equivalent isotropic *U* defined as one-third of the trace of the orthogonalized U_{ij} tensor.

Table III. Atomic Coordinates (×10^4) and Isotropic Thermal Parameters (Å^2 × 10^3) for $Pd_3(\mu_3\text{-}S)_2(S_2C_2O_2)(PMe_3)_4$

	x	*y*	*z*	U^a
Pd(1)	7782.5 (5)	2079	8202.2 (4)	36.8 (2)
Pd(2)	6448.6 (5)	1452.0 (6)	5984.6 (4)	43.9 (2)
Pd(3)	7675.2 (5)	−430.6 (6)	7535.8 (4)	36.8 (2)
S(1)	8711 (2)	1161 (2)	6851 (1)	40 (1)
S(2)	5847 (2)	902 (2)	7568 (1)	43 (1)
S(3)	9591 (2)	−1602 (2)	7463 (2)	55 (1)
S(4)	6538 (2)	−1926 (2)	8238 (2)	57 (1)
P(1)	9936 (2)	2916 (2)	8645 (1)	43 (1)
P(2)	6508 (2)	2700 (2)	9443 (2)	48 (1)
P(3)	7535 (2)	1947 (3)	4600 (2)	68 (1)
P(4)	4147 (2)	1718 (3)	5336 (2)	62 (1)
O(1)	10042 (10)	−3658 (8)	8170 (9)	128 (5)
O(2)	7400 (9)	−4055 (7)	8527 (7)	92 (3)
C(1)	10633 (10)	3633 (9)	7612 (7)	66 (3)
C(2)	11181 (8)	1746 (9)	9025 (8)	73 (4)
C(3)	10272 (10)	3999 (9)	9640 (6)	62 (3)
C(4)	7084 (10)	3768 (11)	10404 (7)	75 (4)
C(5)	4871 (9)	3377 (12)	8920 (8)	87 (4)
C(6)	5974 (13)	1497 (13)	10151 (9)	104 (5)
C(7)	6651 (13)	2267 (27)	3411 (9)	271 (15)
C(8)	8740 (13)	3176 (12)	4907 (9)	100 (5)
C(9)	8753 (15)	893 (13)	4292 (10)	115 (6)
C(10)	3638 (13)	3169 (13)	4998 (14)	135 (7)
C(11)	2861 (9)	1324 (13)	6151 (8)	94 (5)
C(12)	3486 (11)	959 (14)	4190 (9)	97 (5)
C(13)	9194 (10)	−2881 (9)	7992 (6)	62 (3)
C(14)	7678 (10)	−3081 (8)	8281 (6)	63 (3)

[a] Equivalent isotropic *U* defined as one-third of the trace of the orthogonalized U_{ij} tensor.

Table IV. Bond Distances and Angles for I ($(Me_3P)_2Pd(S_2C_2O_2)$)

	(a) Bond Distances (Å)		
Pd–S(1)	2.324 (1)	S(1)–C(1)	1.714 (4)
Pd–S(2)	2.344 (1)	S(2)–C(2)	1.733 (4)
Pd–P(1)	2.294 (1)	C(1)–O(1)	1.217 (5)
Pd–P(2)	2.307 (1)	C(2)–O(2)	1.212 (5)
C(1)–C(2)	1.544 (5)		
	(b) Bond Angles (deg)		
P(1)–Pd–P(2)	95.2 (0)	Pd–S(2)–C(2)	104.7 (1)
P(1)–Pd–S(1)	89.3 (0)	S(1)–C(1)–O(1)	122.8 (3)
P(1)–Pd–S(2)	173.9 (0)	S(2)–C(2)–O(2)	123.4 (3)
P(2)–Pd–S(1)	174.7 (0)	S(1)–C(1)–C(2)	119.2 (3)
P(2)–Pd–S(2)	87.3 (0)	S(2)–C(2)–C(1)	117.9 (3)
S(1)–Pd–S(2)	87.9 (0)	O(1)–C(1)–C(2)	118.0 (4)
Pd–S(1)–C(1)	106.2 (1)	O(2)–C(2)–C(1)	118.6 (4)

Theoretical Studies. Electronic structure calculations of $Pd(C_2O_4)(PH_3)_2$ and $Pd(S_2C_2O_2)(PH_3)_2$ were performed with a DEC-VAX 11/780 minicomputer and used the self-consistent field discrete variational Xα (SCF-Xα-DV) method.[10] Numerical atomic orbitals from exact Hartree–Fock–Slater calculations were used as basis functions, assuming the α values of Schwartz.[11] For palladium, the atomic orbitals through 5p were included. For phosphorus and sulfur, orbitals through 4p were

---

(10) Ellis, D. E.; Painter, G. S. *Phys. Rev. B: Solid State* **1970**, *2*, 2887; Delley, B.; Ellis, D. E. *J. Chem. Phys.* **1982**, *76*, 1949.

(11) Schwartz, K. *Phys. Rev. B: Solid State* **1972**, *5*, 2466.

Table V. Bond Distances and Angles for II ($[(Me_3P)_2Pd]_2(\mu_3\text{-}S)_2Pd(S_2C_2O_2)$)

	(a) Bond Distances (Å)		
Pd(1)–S(1)	2.364 (2)	Pd(1)–P(1)	2.292 (2)
Pd(1)–S(2)	2.374 (2)	Pd(1)–P(2)	2.294 (2)
Pd(2)–S(1)	2.356 (2)	Pd(2)–P(3)	2.307 (2)
Pd(2)–S(2)	2.353 (2)	Pd(2)–P(4)	2.291 (2)
Pd(3)–S(1)	2.333 (2)	S(3)–C(13)	1.705 (10)
Pd(3)–S(2)	2.339 (2)	S(4)–C(14)	1.723 (10)
Pd(3)–S(3)	2.294 (2)	C(13)–C(14)	1.56 (1)
Pd(3)–S(4)	2.306 (2)	C(13)–O(1)	1.22 (1)
Pd(1)···Pd(2)	3.174 (1)	C(14)–O(2)	1.21 (1)
Pd(1)···Pd(3)	3.038 (1)	S(1)···S(2)	3.029 (5)
Pd(2)···Pd(3)	3.141 (1)		
	(b) Bond Angles (deg)		
S(1)–Pd(1)–S(2)	79.5 (1)	S(2)–Pd(3)–S(3)	174.8 (1)
S(1)–Pd(2)–S(2)	80.1 (1)	S(2)–Pd(3)–S(4)	95.5 (1)
S(1)–Pd(3)–S(2)	80.9 (1)	Pd(1)–S(1)–Pd(2)	84.5 (1)
S(3)–Pd(3)–S(4)	89.6 (1)	Pd(1)–S(2)–Pd(2)	84.4 (1)
P(1)–Pd(1)–P(2)	102.8 (1)	Pd(1)–S(1)–Pd(3)	80.6 (1)
P(3)–Pd(2)–P(4)	99.7 (1)	Pd(1)–S(2)–Pd(3)	80.3 (1)
S(1)–Pd(1)–P(1)	88.8 (1)	Pd(2)–S(1)–Pd(3)	84.1 (1)
S(1)–Pd(1)–P(2)	168.1 (1)	Pd(2)–S(2)–Pd(3)	84.0 (1)
S(2)–Pd(1)–P(1)	167.2 (1)	Pd(3)–S(3)–C(13)	106.0 (3)
S(2)–Pd(1)–P(2)	88.7 (1)	Pd(3)–S(4)–C(14)	105.5 (3)
S(1)–Pd(2)–P(3)	87.4 (1)	S(3)–C(13)–O(1)	123.1 (8)
S(1)–Pd(2)–P(4)	172.8 (1)	S(4)–C(14)–O(2)	124.8 (8)
S(2)–Pd(2)–P(3)	167.5 (1)	S(3)–C(13)–C(14)	119.4 (7)
S(2)–Pd(2)–P(4)	92.8 (1)	S(4)–C(14)–C(13)	118.7 (7)
S(1)–Pd(3)–S(3)	94.0 (1)	O(1)–C(13)–C(14)	117.4 (9)
S(1)–Pd(3)–S(4)	176.3 (1)	O(2)–C(14)–C(13)	116.4 (9)

included in the basis. For carbon and oxygen, a minimal 1s, 2s, 2p basis was used. For hydrogen, a 1s, 2s, 2p basis set was used. Core orbitals (1s, ..., 3p for Pd and 1s for C and O) were frozen and orthogonalized against valence orbitals. The Mulliken[12] scheme was used to compute atomic orbital populations. The molecular Coulomb potential was calculated by using a least-squares fit[12] of the model electron density to the true density. Seven radial degrees of freedom were allowed in the expansion of the density, in addition to the radial atomic densities. For the molecular exchange potential, we set $\alpha = 0.701$.

The structure of $Pd(C_2O_4)(PH_3)_2$ was modeled with the bond distances from the X-ray structure[13] of $Pd(C_2O_4)(PEt_3)_2$ idealized to C_{2v} symmetry, assuming P–H = 1.415 Å with ∠H–P–H = 93.8°. In the calculation the same potential function was assumed for all six hydrogens. The structure of $Pd(S_2C_2O_2)(PH_3)_2$ was constructed similarly with the aid of the X-ray structure reported here for $Pd(S_2C_2O_2)(PMe_3)_2$.

Results and Discussion

Bis(phosphine) dithiooxalate complexes of Ni, Pd, and Pt were prepared by metathesis of the corresponding dichloro complex with $K_2S_2C_2O_2$. For Pd and Pt the reaction solvent may be water; however, methanol must be used for the synthesis of nickel compounds. Nonchelating phosphines were susceptible to displacement from nickel and were synthesized by displacing DME from $Ni(S_2C_2O_2)(DME)$. All bis(phosphine) dithiooxalate complexes (Table VI) show a strong absorbance at 1630–1640 cm^{-1} in their IR spectra, which is attributable to the noncomplexed carbonyls of dithiooxalate-*S*,*S*′. Although the single peak found in the ^{31}P NMR spectra (Table VI) supports the structural assignment, there exists the possibility of ionic isomers $[M(PR_3)_4]^{2+}[M(S_2C_2O_2)_2]^{2-}$, which would exhibit similar spectroscopic properties and analyze for the same atomic composition as $M(S_2C_2O_2)(PR_3)_2$. To test for the existence of ionic isomers, conductivity measurements were made for several complexes and were found to be in accord with the monomeric neutral isomer. The X-ray crystal structure of $Pd(S_2C_2O_2)(PMe_3)_2$ was determined and provides a definitive structural identification. All the dithiooxalate complexes are air stable, slightly light sensitive in the solid state, and thermally stable below 50 °C. Their thermal and photochemical sensitivity decreases in the sequence Ni > Pd > Pt. For example, the platinum complexes can be boiled in DMF (152 °C) for days without decomposition, while the palladium and nickel complexes decompose within minutes at this temperature.

Table VI. Spectroscopic Data for Bis(phosphine)nickel, -palladium, and -platinum Chloride and Dithiooxalate Complexes

	X = Cl_2		X = $S_2C_2O_2$		
compd	τ	J_{Pt-P}, Hz	τ	J_{Pt-P}, Hz	$\nu_{C=O}$, cm^{-1}
$NiX(PMe_3)_2$			31.8[a]		1630[e]
$PdX(PMe_3)_2$	−10.5 (trans)[b]		−14.7[b]		1636[f]
$PtX(PMe_3)_2$	−21.8 (cis)[d]	3405[d]	−24.4[a]	2890[a]	1639[f]
NiX(depe)	78.6[a]		75.0[a]		1640[f]
PdX(depe)	88.0[d]		72.8[a]		1632[f]
PtX(depe)	57.5[b]	3546[b]	58.2[a]	2852[a]	1635[f]
NiX(dppe)	57.8[b]		60.1[b]		1638[f]
PdX(dppe)	66.6[d]		59.4[c]		1632[f]
PtX(dppe)	43.1[d]	3598[d]	48.2[d]	2939[d]	1638[f]

[a] CD_3CN. [b] $CDCl_3$. [c] Me_2SO-d_6. [d] DMF/C_6D_6. [e] CH_2Cl_2. [f] CH_3CN.

It has been shown that the oxalate ligand can be thermally and photolytically degraded to yield a reduced metal center plus two molecules of CO_2 gas.[2] It has also been shown that when homoleptic metal dithiooxalate complexes are decomposed photochemically[14] or thermally,[14,15] COS gas is produced. This chemistry might be exploited to generate NiL_2 species that were unavailable through the oxalate photoreactions. Oxalate photoreactions differ from those of dithiooxalates since the oxalates produce inert CO_2 on photolysis while dithiooxalates yield reactive COS. Because the chemistry of COS has been explored as a model for C_1/CO_2 chemistry,[16] the photoreactions of dithiooxalates might provide an alternative method of producing COS within the coordination sphere of zerovalent coordinatively unsaturated metals.

The electronic absorption spectra of the nickel and palladium dithiooxalate complexes show only a decrease in the initial absorbing species on UV photolysis. The platinum complexes show isosbestic behavior, which varies with the solvent used. The irradiation, when performed in CH_3CN, shows isosbestic behavior even at extended photolysis times. In CH_2Cl_2 there is an initial isosbestic point that disappears on continued irradiation. A possible explanation of these results is the initial formation of a solvent-stabilized PtL_2 species or a weakly coordinated COS adduct. Secondary photolysis or thermal decomposition to the dichloride complexes occurs in halogenated solvents. Almost quantitative (90–100%) production of the corresponding metal bis(phosphine) dichlorides occurs (eq 2) on irradiation for extended

$$M(S_2C_2O_2)L_2 \xrightarrow[CH_2Cl_2]{h\nu} MCl_2L_2 \qquad (2)$$

periods in CH_2Cl_2. Attempts to characterize the primary photoproduct (M = Pt) by ^{31}P NMR and IR spectroscopy have shown that the initial photoproduct is either thermally or photochemically unstable. It decomposes on standing, on continued irradiation, or on attempts at isolation. This same instability of primary reaction products is seen for palladium as well. Nickel analogues show different behavior.

When a solution of $Ni(S_2C_2O_2)L_2$ (L_2 = depe or dppe) in CH_3CN is irradiated in an IR cell, an absorption at 2030 cm^{-1} corresponding to free COS grows in immediately. This peak is soon followed by the appearance of new absorptions at 2065, 1990, and 1925 cm^{-1}. These features dominate the spectrum and are attributed to nickel carbonyls. This ability of COS to act as a carbonylating agent toward low-valent transition-metal complexes has been established for V(0),[17] Fe(0),[18] Ru(0),[18] Co(I),[19] Rh(I),[20]

---

(12) Mulliken, R. S. *J. Chem. Phys.* **1955**, *23*, 1833.

(13) Rheingold, A. L.; Yolles, S.; Roat, R.; Fultz, W.; Kretchmar, S. *Acta Crystallogr.*, in press.

(14) Hennig, H.; Kumpt, W.; Jurdeczka, K.; Benedix, R. *J. Prakt. Chem.* **1977**, *319*, 444.

(15) Imamura, T.; Ryan, M.; Gordon, G.; Coucouvanis, D. *J. Am. Chem. Soc.* **1984**, *106*, 984.

(16) Ibers, J. A. *Chem. Soc. Rev.* **1982**, *11*, 57.

(17) Pasquali, M.; Floriani, C.; Chiesi-Villa, A.; Guastini, C. *Inorg. Chem.* **1980**, *19*, 3847. Gambarotta, S.; Fiallo, M. L.; Floriani, C.; Chiesi-Villa, A.; Guastini, C. *Inorg. Chem.* **1984**, *23*, 3532.

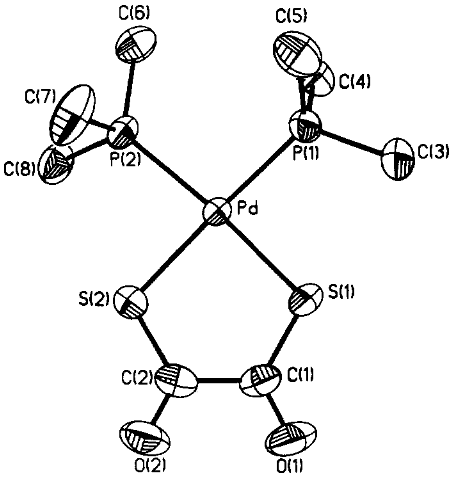

Figure 1. Thermal ellipsoid diagram and labeling scheme for I ((dithiooxalato-*S*,*S*′)bis(trimethylphosphine)palladium(II)).

Ni(0),[21] and Pt(0).[22] Sulfur often is trapped as phosphine sulfide,[18,20a] forms complexes with the metals themselves,[17,18,20b,21,22] or remains unidentified,[19,21b] as in the present case.

The ability of COS to act as a carbonylating agent accounts for the appearance of nickel carbonyls, but its total isolated yield is only 5–10%. A ^{31}P NMR spectrum of the crude photolysis solution of $Ni(dppe)(S_2C_2O_2)$ in CH_3CN showed a resonance corresponding to monomeric $Ni(dppe)(CO)_2$ as compared with spectra of authentic samples.[23] There was an additional species consisting of two doublets (δ = 43.89 and 27.46; J = 54 Hz). Attempts to isolate this product from the photolysis mixture have resulted in decomposition. This ^{31}P NMR spectrum could be explained by a $Ni(dppe)(\eta^2\text{-}COS)$ complex.

To see whether the photoreaction of $Ni(S_2C_2O_2)(dppe)$ yields products expected from the reaction between nickel(0) phosphine complexes and COS we examined the reaction between $Ni(dppe)_2$ and COS in nonpolar solvents. A complex reaction occurs to yield a variety of products, which include the $Ni(dppe)(CO)_2$ seen in the photoreaction. Ibers and Gaffney[21b] observed a similar reaction between $Ni(PPh_3)_4$ and COS. If the reaction is performed in a more polar solvent (acetone or THF), a clean transformation of the $Ni(dppe)_2$ to the same species (pair of ^{31}P doublets) seen in the photochemical reaction was observed.

Since the same metal species forms in the photochemical and thermal reactions it suggests that the photochemistry of these metal bis(phosphine) dithiooxalates proceeds through a coordinatively unsaturated zerovalent species and that this intermediate reacts with available COS gas to yield the observed products. Unfortunately, all attempts to isolate products by removal of solvent or precipitation results in decomposition.

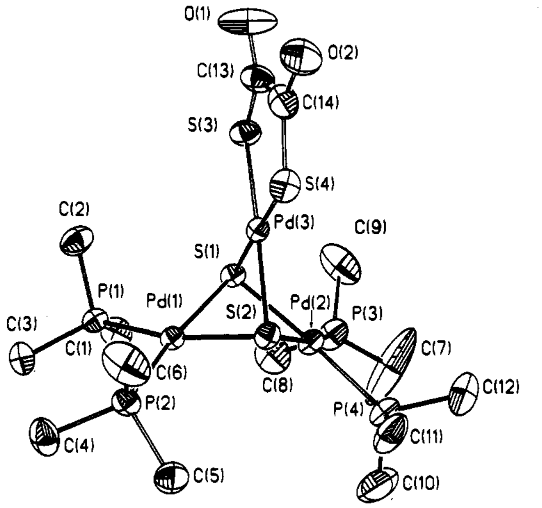

Figure 2. Thermal ellipsoid diagram and labeling scheme for II ((1,1-dithiooxalato-*S*,*S*′)bis(μ_3-sulfido)-2,2,3,3-tetrakis(trimethylphosphine)-*triangulo*-tripalladium(II)).

Table VII. Least-Squares Plane Calculations for I and II

Complex I

atom	dev, Å	atom	dev, Å
Plane I: $0.7763X + 0.6298Y - 0.0288Z - 1.9828 = 0$			
Pd	−0.0651	P(1)	0.0454
S(1)	−0.0139	P(2)	−0.0119
S(2)	0.0454		

Plane I: Pd, S(1), S(2), P(1), P(2)

Complex II

atom	dev, Å	atom	dev, Å
Plane I: $0.3231X - 0.7691Y + 0.5515Z - 6.1680 = 0$			
Pd(1)	−0.0628	P(1)	0.0444
S(1)	−0.0179	P(2)	−0.0091
S(2)	0.0454		
Plane II: $0.0411X + 0.9554Y + 0.2924Z - 4.0000 = 0$			
Pd(2)	−0.0153	P(3)	−0.0051
S(1)	0.0140	P(4)	0.0131
S(2)	−0.0066		
Plane III: $0.3820X + 0.2960Y + 0.8755Z - 10.7161 = 0$			
Pd(3)	−0.0116	S(3)	0.0040
S(1)	0.0018	S(4)	0.0021
S(2)	0.0038		

Plane I: Pd(1), S(1), S(2), P(1), P(2)
Plane II: Pd(2), S(1), S(2), P(3), P(4)
Plane III: Pd(3), S(1), S(2), S(3), S(4)

Dihedral Angles (deg) between Planes

	II	III
I	124.1	112.2
II		123.7

Discussion of X-ray Structures. The structure determination of $Pd(S_2C_2O_2)(PMe_3)_2$ (I) shows the sulfur-bound dithiooxalate ligand and a square-planar coordination geometry about palladium (Figure 1). Slight deviations from 90° angles (Table IV) can be attributed to the steric repulsions of the two cis phosphine ligands coupled to the chelation of the dithiooxalate moiety. In comparison to the $Pd(C_2O_4)(PEt_3)_2$ structure,[13] most structural parameters of I are consistent with expectations based on the S-for-O substitution; e.g., the O–Pd–O angle in $Pd(C_2O_4)(PEt_3)_2$ opens from 81.1 (1)° to 87.9 (0)° for the S–Pd–S angle in I to accommodate the wider bite of the dithiooxalate ligand. The most noteworthy difference in the two structures is a significant lengthening of the Pd–P distances for I: 2.253 (1) Å (average) for $Pd(C_2O_4)(PEt_3)_2$, and 2.301 (1) Å (average) for I. The difference suggests that the thiooxalate ligand is a better translabilizing group than oxalate, which is consistent with the theoretical studies discussed below.

The geometry of II can be thought of as a triangle of Pd atoms capped on top and bottom by triply bridging sulfide ligands (Figure 2). Similar structures have been observed for the entire triad Ni,[24] Pd,[25] and Pt.[26] These three palladium and two bridging

---

(18) Gaffney, T. R.; Ibers, J. A. *Inorg. Chem.* **1982**, *21*, 2851.

(19) Bianchini, C.; Meli, A.; Scapacci, G. *Organometallics* **1983**, *2*, 1834.

(20) (a) Datta, S.; Pandey, K. K.; Agarwala, U. C. *Inorg. Chim. Acta* **1980**, *40*, 65. (b) Gaffney, T. R.; Ibers, J. A. *Inorg. Chem.* **1982**, *21*, 2857.

(21) (a) Poppitz, W.; Uhlig, E. *Z. Anorg. Allg. Chem.* **1982**, *489*, 67. (b) Gaffney, T. R.; Ibers, J. A. *Inorg. Chem.* **1982**, *21*, 2860. (c) Poppitz, W.; Uhlig, E. *Z. Chem.* **1979**, *19*, 191.

(22) Baird, M. C.; Wilkinson, G. *J. Chem. Soc. A* **1967**, 865. Skapski, A. C.; Troughton, P. G. H. *J. Chem. Soc. A* **1969**, 2772.

(23) Follow the procedure described using dppe in place of PPh_3: Giannoccaro, P.; Sacco, A.; Vasapollo, G. *Inorg. Chim. Acta* **1979**, *37*, L455.

(24) Vahrenkamp, H.; Uchtman, V. A.; Dahl, L. F. *J. Am. Chem. Soc.* **1968**, *90*, 3272. Orlandini, A.; Battistoni, C.; Mattogno, G. *J. Chem. Soc., Dalton Trans.* **1984**, 939.

Table VIII. Reduction Waves in Cyclic Voltammograms of Nickel, Palladium, and Platinum Bis(phosphine) Oxalate and Dithiooxalate Complexes

compd	$E_{p,c}$,[a] V	$E_{p,a}$, V	ΔE_p, mV	$i_{p,c}/i_{p,a}$	E_0', V
$Ni(S_2C_2O_2)(dppe)$	−1.18	−1.10	87	1.20	−1.14
$Pd(S_2C_2O_2)(dppe)$	−1.45	IRR[b]			
$Pt(S_2C_2O_2)(dppe)$	−1.58	−1.49	93	0.88	−1.54
$Ni(S_2C_2O_2)(depe)$	−1.53	−1.41	122	0.87	−1.47
$Pd(S_2C_2O_2)(depe)$	−1.73	−1.58	153	1.26	−1.66
$Pt(S_2C_2O_2)(depe)$	−1.72	−1.61	109	1.08	−1.67
$Ni(S_2C_2O_2)(PMe_3)_2$	−1.17	IRR			
$Pd(S_2C_2O_2)(PMe_3)_2$	−1.49	IRR			
$Pt(S_2C_2O_2)(PMe_3)_2$	−1.66	−1.57	95	1.25	−1.62
$Pd(C_2O_4)(PEt_3)_2$	−1.51	IRR			
$Pt(C_2O_4)(PMe_3)_2$	−1.81	IRR			
$Pt(C_2O_4)(PEt_3)_2$	−2.09	IRR			
$Fe(\eta\text{-}C_5H_5)_2$	+0.19	+0.30	113	1.00	0.246

[a] All measurements were for 1 mM solutions of the complex that contained 0.1 M $(Bu_4N)ClO_4$ in CH_3CN at a 200 mV/s scan rate. A Pt working electrode and a Ag/AgCl reference electrode were used. [b] IRR denotes an irreversible reduction wave.

sulfur atoms form a trigonal-bipyramidal structure distorted on one side by having one Pd–Pd distance anomalously shorter than the other two (3.038 (1) Å compared to 3.141 (1) and 3.174 (1) Å). The coordination geometry about each palladium approximates a square plane (Table VII). Dihedral angles of 124.1 and 123.7° were observed between the planes containing Pd(1) and Pd(2) and the planes containing Pd(2) and Pd(3), respectively. A smaller angle, 112.2°, was found between the coordination planes containing Pd(1) and Pd(3). A similar distortion was seen[25] in a crystal of $[Pd_3(\mu_3\text{-}S)_2(PMe_3)_6]^{2+}$ where the short Pd–Pd bond distance was 3.011 (2) Å compared to 3.144 (2) and 3.178 (2) Å. The cause for this distortion in the totally symmetric dication is unknown.

The coordination geometry around each Pd atom is nearly square planar with the expected angle opening to ~100° between the phosphines and resultant closing to ~80° between the bridging sulfurs. For Pd(1) and Pd(2), which contain PMe_3 ligands, there is a slight distortion from planarity that displaces trans ligands out of the plane in the same direction, but the orthogonal pairs of trans ligands are displaced in opposite directions, with respect to the least-squares planes. The parent complex, $Pd(S_2C_2O_2)(PMe_3)_2$, exhibits a similar distortion (Table VII) that probably results from crowding of the cis phosphine ligands. For Pd(3) in II, which does not have bound PMe_3 ligands, the distortion from planarity is much less. Thus, as we have argued previously[27] from cis–trans equilibrium data for PtH_2L_2 (L = PEt_3 and PMe_3), even the PMe_3 complexes show effects of steric crowding.

When structures I and II are compared, the greater trans-directing influence of the PMe_3 group as compared to bridging sulfide becomes apparent. Thus the Pd–S bond distance in complex I (2.334 Å, average) exceeds that in II (2.200 Å, average). In a comparison of other bond lengths, the Pd—P, C—C, and C=O distances are similar in both cases.

Electrochemistry. Cyclic voltammetry measurements for the reductions of several bis(phosphine) dithiooxalate and oxalate complexes are summarized in Table VIII. Analysis of this data demonstrates the following: all oxalate complexes exhibit chemically irreversible reductions; all platinum bis(phosphine) dithiooxalates show chemically reversible reductions; all depe dithiooxalates show some degree of chemical reversibility; of the remaining dithiooxalate complexes, only $Ni(S_2C_2O_2)(dppe)$ (reported previously[4]) showed any sign of reversible behavior; the ease of reduction follows the order Ni > Pd ≥ Pt. Controlled-potential coulometry measurements for $Pt(S_2C_2O_2)(depe)$ show 0.95 ± 0.1 electron transferred in the reduction.

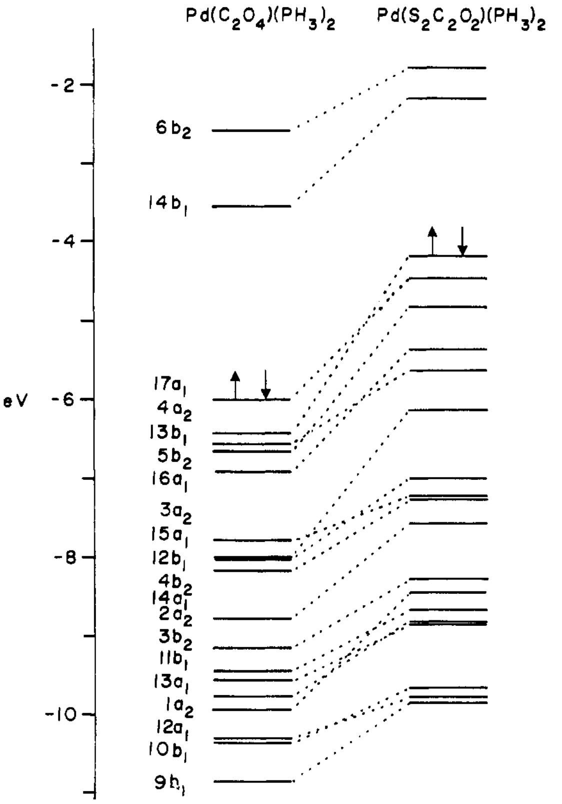

Figure 3. Molecular orbital diagrams from SCF–Xα–DV calculations for $Pd(O_2C_2O_2)(PH_3)_2$ and $Pd(S_2C_2O_2)(PH_3)_2$.

As expected, Ni(II) is easier to reduce than Pd(II) or Pt(II), which reflects the increasing stability of the d^8 square-planar structure as the crystal field strength increases on descending a metal triad. The energy difference between a square-planar d^8 ML_4 and a d^9 ML_4^- species should have a large crystal field component. The greater stability (i.e. chemical reversibility in the cyclic voltammogram) of the reduced dithiooxalate complexes may also reflect the ability of soft ligands to delocalize electrons. That the complexes containing depe exhibit the greatest stability suggests that phosphine dissociation in the reduced complexes may aid their decomposition. Of the phosphorous ligands studied, chelating depe is expected to bind most tightly to metals.

Theoretical Studies. To define the electronic similarities between metal oxalate and dithiooxalate complexes as well as to define the low-energy photoactive excited states in these complexes we performed SCF–Xα–DV calculations on the model complexes $Pd(C_2O_4)(PH_3)_2$ and $Pd(S_2C_2O_2)(PH_3)_2$. The valence orbitals and energies (Figure 3, Table IX) for the two complexes are similar, except that those of the dithiooxalate complex are destabilized as compared to the corresponding oxalate species. The $13b_1$, $12b_1$, and $1a_2$ orbitals, which show the most destabilization, involve either the anionic chelate orbitals ($13b_1$ and $12b_1$) or a change in bonding character (e.g. $1a_2$ shows little binding to dithiooxalate).

The more positive calculated atomic charge (Table X) of phosphorus in the oxalate complex as compared to that in the dithiooxalate complex suggests phosphorus donates more electrons (i.e. binds better) to Pd in the oxalate complex. This agrees with the shorter Pd–P bonds in $Pd(C_2O_4)(PEt_3)_2$ as compared to $Pd(S_2C_2O_2)(PEt_3)_2$. The atomic charge for sulfur in the dithiooxalate complex compared with that for Pd-bound oxygen in the oxalate complex shows dithiooxalate to be a better donor. This also agrees with the previous conclusion that dithiooxalate exhibits a larger trans effect than oxalate. It is interesting that the decreased charge donation from P compensates the increased donor ability of S in the dithiooxalate complex. Thus the Pd charges (Table X) calculated are nearly the same in both complexes. The similar reduction potentials observed (Table VIII) for palladium oxalate

---

(25) Werner, H.; Bertleff, W.; Schubert, U. *Inorg. Chim. Acta* **1980**, *43*, 199.
(26) Chatt, J.; Mingos, D. M. P. *J. Chem. Soc. A* **1970**, 1243.
(27) Packett, D. L.; Jensen, C. M.; Cowan, R. L.; Strouse, C. E.; Trogler, W. C. *Inorg. Chem.* **1985**, *24*, 3578.

Table IX. Percent Atomic Compositions (>5%) of the Valence Orbitals from SCF–Xα–DV Calculations

	$Pd(C_2O_4)(PH_3)_2$							$Pd(S_2C_2O_2)(PH_3)_2$						
		% composition							% composition					
orbital	energy, eV	Pd	P	O_b	O	C	H	energy, eV	Pd	P	S	O	C	H
$9b_1$	−10.86	39	9	9	22	5		−9.84	47	13		18		12
$10b_1$	−10.36	9	7	20	40	9	6	−9.66		35		12		47
$12a_1$	−10.30	14	40		12		32	−9.78	8	14		57	14	
$1a_2$	−9.95	23		26	23	26		−8.49	33	19		18	12	15
$13a_1$	−9.75	44	16	13	7	5	13	−8.83	14	20	15	13	15	16
$11b_1$	−9.57		37				56	−8.85		15	27	32	14	9
$3b_2$	−9.46	72	13				8	−8.68	27	33				39
$2a_2$	−9.16	56	10		19	11		−8.28	9	14		42	22	12
$14a_1$	−8.78	60	19		5		8	−7.60	80	5				5
$4b_2$	−8.17	18	33	5	5		38	−7.29	66	10				18
$12b_1$	−8.00		13	48	25	5		−6.18			26	61	10	
$15a_1$	−8.00	45	40				11	−6.99	72	16	77			7
$3a_2$	−7.84	15	35				45	−7.23	53	14				28
$16a_1$	−6.93	20			72			−5.34	14		67	10		
$5b_2$	−6.67	11		23	44	32		−4.82	10		61	23		
$13b_1$	−6.57		13	18	60			−5.63	21	19	26	20		9
$4a_2$	−6.43	10		57	32			−4.19[a]	6		77	15		
$17a_1$	−6.10[a]			17	65	16		−4.46			25	53	17	
$14b_1$	−3.55	19	24	33	5		18	−2.11	15	10	50	6		16
$6b_2$	−2.59			23	44	32		−1.77	14	9	13	30	25	7

[a] Highest filled orbital.

Table X. Mulliken-like Population Analyses

$Pd(C_2O_4)(PH_3)_2$		$Pd(S_2C_2O_2)(PH_3)_2$	
atom	charge	atom	charge
Pd	−0.255	Pd	−0.242
P	+0.392	P	+0.354
O(Pd)	−0.223	S	−0.013
O	−0.255	O	−0.236
C	+0.293	C	+0.083
H	−0.027	H	−0.022

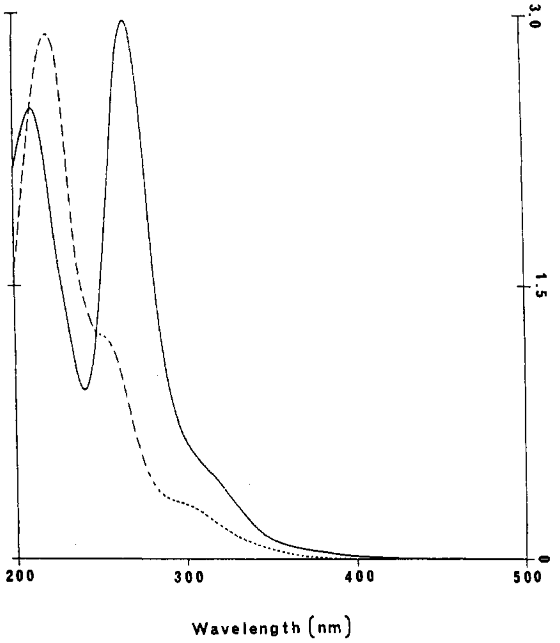

Figure 4. Electronic absorption spectra of $Pd(C_2O_4)(PEt_3)_2$ (- - -) and $Pd(S_2C_2O_2)(PMe_3)_2$ (—), both 1.02 × 10^{-4} M in CH_3CN solution.

and dithiooxalate derivatives support this conclusion.

The lowest excited states in both complexes should arise from one-electron transitions from the $C_2O_4^{2-}$- or $C_2O_2S_2^{2-}$-localized orbitals ($17a_1$ or $4a_2$, a π level) to $6b_2$, an orbital with $C_2O_4^{2-}$ or $C_2O_2S_2^{2-}$ π^* character and some admixture of Pd, or to $14b_1$. Thus the intuitive qualitative description of the photoactive transitions as ligand to metal charge transfer, which we proposed[2] previously to explain the photoreductive elimination, is not appropriate. Localization of excitation energy on the ligand is also consistent with the photofragmentation character of the reductive-elimination reactions. Aside from an intensity increase in the dithiooxalate complex, the absorption spectra (Figure 4) of $Pd(C_2O_4)(PEt_3)_2$ and $Pd(S_2C_2O_2)(PEt_3)_2$ closely resemble one another, as expected from the calculated energy levels. Although it is difficult to make unambiguous band assignments on the basis of the information available, the similarity of the HOMO-LUMO gap (without relaxation) from the calculations (2.5 eV for $Pd(C_2O_4)(PEt_3)_2$ and 2.1 eV for $Pd(S_2C_2O_2)(PEt_3)_2$) is reflected in the similarity of the first absorption band energy, ca. 300 nm (4.13 eV), in the two complexes. Orbital relaxation effects usually add an additional 2 eV to the energy gap from ground-state calculations.[28] Therefore, the calculations give reasonable estimates for the transition energy as well.

Acknowledgment. This research was supported by the U.S. Army Research Office under contract DAAG29-85-K-0263 to W.C.T. Funds supporting the purchase of the University of Delaware diffractometer were provided by the NSF. We gratefully acknowledge Johnson Matthey, Inc., for a loan of precious metals under their University Metal Loan Program. Helpful discussions with Prof. Fred Basolo are gratefully acknowledged.

Supplementary Material Available: Tables of bond lengths (Tables 2S and 7S), bond angles (Tables 3S and 8S), anisotropic thermal parameters (Tables 4S and 9S), and hydrogen atom coordinates and isotropic thermal parameters (Tables 5S and 10S) for I and II (6 pages); tables of observed and calculated structure factors (Tables 1S and 6S) for I and II (28 pages). Ordering information is given on any current masthead page.

---

(28) Holland, G. F.; Ellis, D. E.; Trogler, W. C. *J. Am. Chem. Soc.* **1986**, *108*, 1884.